Vol. 92 No. 5 pp. 2043–2045 ACTA GEOLOGICA SINICA (English Edition) Oct. 2018

Research Advances

A New Discovery of ~3.0 Ga Tonalitic Gneiss in Northern Liaoning Province, China

LI Zhuang[1, 2, *], LIU Jin[3], WEI Chunjing [4] and CHEN Bin[5]

1 *State Key Laboratory of Petroleum Resources and Prospecting, China University of Petroleum (Beijing), Beijing 102249, China*
2 *College of Geosciences, China University of Petroleum (Beijing), Beijing 102249, China*
3 *School of Earth Sciences and Engineering, Sun Yat-Sen University, Guangzhou 510275, China*
4 *School of Earth and Space Sciences, Peking University, Beijing 100871, China*
5 *School of Resources and Environmental Engineering, Hefei University of Technology, Hefei 230009, China*

Objective

The North China Craton, bounded by the Paleozoic Central Asian Orogenic Belt on the north and by the Qinling–Dabie–Su–Lu Orogenic Belt on the south, is one of the oldest continental nuclei on Earth as a consequence of its preservation of some of the oldest rock records ranging up to ca. 3.85 Ga and mineral older than 4.0 Ga (Li et al., 2016, 2017). Ancient zircons have been extensively reported from different parts of the craton, but Eoarchean–Mesoarchean rocks are only exposed in Anshan of Eastern Liaoning Province and Eastern Hebei Province based on SHRIMP, LA-ICP-MS and SIMS U-Pb isotopic dating of zircons. For the first time, we report the occurrence of a 3.0 Ga tonalitic gneiss (sample No. 15Q22 -2) from the Luanjiajie Village in Fushun City, Northern Liaoning Province, China (GPS location: 42°25′26′′N, 124°48′23′′E), which is also newly revealed as a Mesoarchean lithotectonic element outside Eastern Liaoning Province and Eastern Hebei Province and the oldest rock recognized in Northern Liaoning Province so far.

Methods

The zircon grains were extracted from the sample using heavy liquid and magnetic methods and were further purified by handpicking under a binocular microscope. The zircon grains were set in an epoxy mount that was polished and then vacuum coated with a layer of 50 nm high-purity gold. Cathodoluminescence (CL) images were taken to examine the internal structure of the individual grains. The zircon U-Pb analysis was performed using the LA-ICP-MS housed at the Laboratory Center, Xi'an Center of the Geological Survey, Xi'an, China.

Results

(1) The Mesoarchean tonalitic gneisses occur as enclaves in early Mesozoic granitoids (ca. 160 Ma based on our new SIMS U-Pb isotopic dating of zircons). The tonalitic gneisses have a mineral assemblage of plagioclase (>60%), quartz (15%–25%), hornblende (5%–10%), microcline (< 5%), and biotite (<5%), along with accessory zircon, apatite, titanite, and magnetite. All the minerals are generally <2 mm in size. The tonalitic gneisses have undergone intense deformation and metamorphism that generated a mineral-defined preferred orientation and irregular grain boundaries, all of which are indicative of plastic deformation. Most of the biotite and hornblende have a shape preferred orientation that helps defines the gneissosity, although minor amounts are oblique to themain fabric. These tonalitic gneisses contain alternating light and dark bands that are defined by variations in the composition and abundance of minerals. The light bands (1–10 cm) are wider than the darker bands and contain quartz and plagioclase, whereas the dark bands (0.5–3 cm wide) contain biotite and hornblende. In addition to the banded structure, the gneisses also commonly contain ptygmatic and sheath folds that formed during plastic deformation. They have undergone amphibolite-facies metamorphism, and there are no relict orthopyroxenes or textural evidence (such as blebby textured pseudomorphs of biotite ± hornblende after pyroxene) that would indicate an episode of granulite-facies metamorphism

* Corresponding author. E-mail: lizhuangcc@pku.edu.cn; lizhuangcc@126.com

(2) The CL images of representative zircons (Fig. 1) give insights into the genesis of these zircons and the resulting U–Pb data (Appendix 1), which in turn constrains the magmatic precursor and metamorphic ages of the host rocks. They are pale yellow in color and generally subhedral to euhedral columnar in shape, with long axes of 80 –150 mm in length. These zircons commonly have core–rim structures visible in CL images and contain grey cores with visible oscillatory growth zoning and striped absorption, both of which are indicative of a magmatic origin. In comparison, the dark rims of these zircons have blurred irregular banding and zoning that is indicative of recrystallization during metamorphism, despite the metamorphic rims of variable widths.

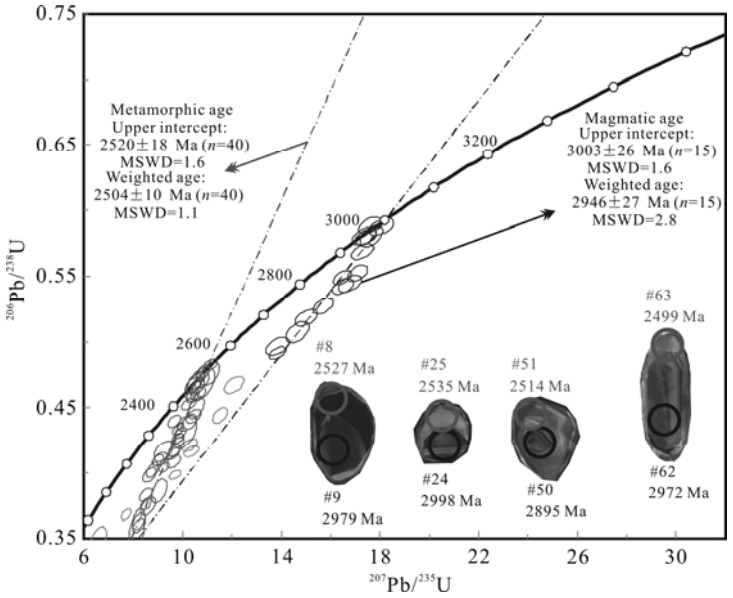

Fig 1. U-Pb zircon concordia diagrams and CL images for representative zircons from the Mesoarchean tonalitic gneiss (15Q22-2).

(3) Sixty-eight analyses of zircons were obtained from this sample. All the magmatic zircon core analyses define an upper intercept age of 3003±26 Ma (MSWD=1.6, *n*=15), which is consistent with the $^{207}Pb/^{206}Pb$ weighted mean age of 2946±27 Ma (2835–2998 Ma; MSWD=2.8, *n*=15). All the zircon rim analyses define an upper intercept age of 2520±18 Ma (MSWD=1.6, *n*=40), which is consistent with the $^{207}Pb/^{206}Pb$ weighted mean age of 2504 ± 10 Ma (2421–2558 Ma; MSWD=1.1, *n*=40) obtained from almost concordant zircons (Fig. 1). We consider that the precursor of the tonalitic gneiss (15Q22-2) was emplaced at 3.0 Ga and was then modified during a metamorphic event at 2.5 Ga (Fig. 1). Spots with the youngest age, such as 2.3–2.2 Ga, are interpreted as having been produced during later metamorphism or alteration events.

(4) The U-Pb isotopic data for zircons from the tonalitic gneisses reveals an emplacement age of ca. 3.0 Ga in this contribution. An amphibolite intercalated with the tonalitic gneiss suggests that magmatic precursors of the amphibolite took place no later than 3.0 Ga. However, we were not able to unequivocally distinguish whether the amphibolite was coeval with or older than the tonalitic gneiss, because they both underwent amphibolite-facies metamorphism and extensive deformation, and not enough zircons were obtained from the amphibolite to identify the age of its protolith. The amphibolite is dominated by plagioclase and hornblende along with minor quartz that formed during migmatization and defines a myrmekitic texture.

Conclusions

A Mesoarchean tonalitic gneiss was identified in Northern Liaoning Province, China, which is also newly reported as an ancient lithotectonic element outside Eastern Liaoning Province and Eastern Hebei Province. U-Pb isotopic dating using the LA-ICP-MS method on zircons from the tonalitic gneissreveals that its magmatic precursor was emplaced at ca. 3.0 Ga and was subjected to subsequent ca. 2.5 Ga metamorphism. This study may also indicate that the possibility of discovering additional ancient rocks from other outcrops and drill holes in the North China Craton.

Acknowledgments

This research was financially supported by the National Science Foundation of China (grants No. 41430207 and 90914001).

References

Li Zhuang, Chen Bin and Wang Jialin, 2016. Geochronological framework and geodynamic implications of mafic magmatism in the Liaodong Peninsula and adjacent regions, North China Craton. *Acta Geologica Sinica* (English Edition), 90(1): 138–153.

Li Zhuang, Wei Chunjing and Chen Bin, 2017. The first discovery of Hadean zircon in the Paleoproterozoic rock. *Acta Geologica Sinica* (English Edition), 91(6): 2321–2323.

Appendix 1 Zircon U-Pb age data

Spot	Th (ppm)	U (ppm)	Th/U	Isotopic ratios						Corrected ages (Ma)						Disc (%)
				$^{207}Pb/^{206}Pb$	1σ	$^{207}Pb/^{235}U$	1σ	$^{206}Pb/^{238}U$	1σ	$^{207}Pb/^{206}Pb$	1σ	$^{207}Pb/^{235}U$	1σ	$^{206}Pb/^{238}U$	1σ	
Magmatic zircon																
15Q22-2-06	302.44	200.26	1.51	0.216286	0.003965	17.371915	0.322760	0.580604	0.004543	2953	30	2956	18	2951	19	0.07
15Q22-2-09	488.80	276.41	1.77	0.219824	0.003765	17.293647	0.300554	0.568872	0.003892	2979	27	2951	17	2903	16	2.56
15Q22-2-20	466.39	385.53	1.21	0.213754	0.004035	15.698069	0.276954	0.527155	0.003895	2934	31	2859	17	2729	17	6.98
15Q22-2-24	264.38	255.95	1.03	0.222324	0.003702	17.090619	0.270604	0.552329	0.004140	2998	26	2940	15	2835	17	5.44
15Q22-2-38	140.65	862.23	0.16	0.202947	0.003470	13.847185	0.225750	0.491186	0.003095	2850	28	2739	16	2576	13	9.63
15Q22-2-43	284.59	271.75	1.05	0.200927	0.004468	13.859305	0.316226	0.496401	0.004669	2835	36	2740	22	2598	20	8.35
15Q22-2-44	2336.37	1348.40	1.73	0.221387	0.004215	18.053888	0.337050	0.587575	0.004226	2991	30	2993	18	2980	17	0.38
15Q22-2-45	990.99	625.30	1.58	0.215347	0.003810	17.591325	0.301292	0.588650	0.004253	2946	29	2968	17	2984	17	-1.29
15Q22-2-48	930.10	639.50	1.45	0.221970	0.004053	16.787711	0.305955	0.544458	0.004271	2995	30	2923	18	2802	18	6.43
15Q22-2-49	79.52	650.03	0.12	0.208200	0.004270	14.658197	0.309379	0.507265	0.005388	2892	33	2793	20	2645	23	8.53
15Q22-2-50	186.36	516.04	0.36	0.208576	0.004194	15.019490	0.299776	0.518145	0.004201	2895	33	2816	19	2691	18	7.03
15Q22-2-60	302.41	307.78	0.98	0.215850	0.003314	16.473437	0.241504	0.549011	0.003612	2950	25	2905	14	2821	15	4.36
15Q22-2-61	279.40	297.87	0.94	0.216107	0.003726	17.421892	0.283396	0.579984	0.004016	2954	28	2958	16	2949	16	0.17
15Q22-2-62	147.95	192.70	0.77	0.218882	0.004074	16.501351	0.288178	0.542227	0.003970	2973	30	2906	17	2793	17	6.05
15Q22-2-66	310.57	269.02	1.15	0.219114	0.003849	17.653886	0.309279	0.580686	0.005375	2976	28	2971	17	2952	22	0.82
Metamorphic zirocn																
15Q22-2-02	45.69	80.73	0.57	0.163213	0.003139	10.252794	0.193540	0.452814	0.002932	2500	32	2458	18	2408	13	3.69
15Q22-2-03	40.34	58.53	0.69	0.167266	0.002859	9.680384	0.166860	0.417466	0.003019	2531	29	2405	16	2249	14	11.16
15Q22-2-04	126.75	328.93	0.39	0.163915	0.002692	10.828384	0.178870	0.476787	0.003584	2498	27	2509	15	2513	16	-0.60
15Q22-2-05	26.48	39.99	0.66	0.158626	0.002543	9.000694	0.149215	0.409719	0.002846	2443	27	2338	15	2214	13	9.37
15Q22-2-08	34.51	50.29	0.69	0.166936	0.003133	10.640675	0.204083	0.460823	0.003226	2527	31	2492	18	2443	14	3.31
15Q22-2-10	85.23	66.27	1.29	0.166191	0.002584	9.804298	0.153221	0.426414	0.002507	2519	25	2417	14	2290	11	9.13
15Q22-2-11	15.89	11.07	1.44	0.158039	0.002839	8.774666	0.160356	0.402020	0.003663	2435	30	2315	17	2178	17	10.54
15Q22-2-12	289.42	210.39	1.38	0.166221	0.002731	9.813664	0.158038	0.426301	0.002665	2520	27	2417	15	2289	12	9.17
15Q22-2-13	11.93	10.75	1.11	0.167029	0.003057	9.794689	0.173496	0.423183	0.002891	2528	30	2416	16	2275	13	10.01
15Q22-2-14	121.63	101.27	1.20	0.170041	0.003423	9.634037	0.189176	0.408675	0.003258	2558	34	2400	18	2209	15	13.66
15Q22-2-15	8.39	11.41	0.74	0.169660	0.003475	10.450585	0.210911	0.443594	0.003534	2554	34	2476	19	2367	16	7.33
15Q22-2-16	61.42	76.98	0.80	0.166603	0.002985	9.603788	0.169348	0.414861	0.002969	2524	29	2398	16	2237	14	11.36
15Q22-2-17	15.55	25.82	0.60	0.163248	0.003184	8.236906	0.166684	0.363133	0.004287	2500	32	2257	18	1997	20	20.12
15Q22-2-18	29.19	37.45	0.78	0.159673	0.003367	8.504105	0.170954	0.383170	0.003294	2454	35	2286	18	2091	15	14.78
15Q22-2-21	35.69	53.14	0.67	0.159934	0.003360	10.424248	0.204247	0.467413	0.003929	2455	35	2473	18	2472	17	-0.69
15Q22-2-22	21.16	31.71	0.67	0.164338	0.003521	8.227064	0.156697	0.359597	0.003436	2502	36	2256	17	1980	16	20.85
15Q22-2-23	42.99	57.55	0.75	0.166368	0.003246	7.816547	0.181931	0.335598	0.003941	2521	33	2210	21	1865	19	26.01
15Q22-2-25	25.04	37.67	0.66	0.167742	0.003281	10.120585	0.298418	0.431298	0.008272	2535	33	2446	27	2312	37	8.83
15Q22-2-26	64.33	84.63	0.76	0.163760	0.002753	10.599953	0.178468	0.466277	0.004674	2495	29	2489	16	2467	21	1.10
15Q22-2-27	78.98	65.72	1.20	0.168214	0.002698	10.546947	0.214060	0.450121	0.005568	2540	27	2484	19	2396	25	5.67
15Q22-2-29	9.91	8.83	1.12	0.168221	0.005729	8.144024	0.219139	0.355414	0.011688	2540	56	2247	24	1960	56	22.81
15Q22-2-30	38.12	244.20	0.16	0.161873	0.002945	10.494362	0.193201	0.468279	0.005016	2476	31	2479	17	2476	22	-0.02
15Q22-2-31	74.49	438.06	0.17	0.164318	0.002426	10.651633	0.166838	0.467005	0.004113	2502	25	2493	15	2470	18	1.26
15Q22-2-32	9.56	9.10	1.05	0.164663	0.002462	9.245205	0.134064	0.404341	0.002551	2506	25	2363	13	2189	12	12.63
15Q22-2-33	218.47	144.41	1.51	0.163185	0.002509	10.407672	0.161213	0.459389	0.003605	2500	26	2472	14	2437	16	2.53
15Q22-2-39	186.57	1651.04	0.11	0.167213	0.004029	10.194332	0.262009	0.438655	0.004205	2531	35	2453	24	2345	19	
15Q22-2-40	46.27	309.66	0.15	0.156721	0.003380	8.662315	0.180854	0.398426	0.003705	2421	36	2303	19	2162	17	10.70
15Q22-2-42	29.55	1114.53	0.03	0.159523	0.004324	9.215205	0.250157	0.416581	0.005149	2450	45	2360	25	2245	23	8.38
15Q22-2-46	15.44	1728.23	0.01	0.158611	0.002885	9.676371	0.171424	0.439684	0.003134	2443	31	2404	16	2349	14	3.82
15Q22-2-51	48.42	96.51	0.50	0.165615	0.003887	8.606021	0.196265	0.374512	0.004605	2514	40	2297	21	2051	22	18.43
15Q22-2-53	149.22	347.70	0.43	0.165258	0.002968	10.786461	0.188200	0.470494	0.003817	2510	30	2505	16	2486	17	0.97
15Q22-2-54	93.37	159.19	0.59	0.165806	0.002419	9.924081	0.138998	0.430862	0.002604	2517	24	2428	13	2310	12	8.23
15Q22-2-55	46.53	72.66	0.64	0.163239	0.002468	9.828303	0.146195	0.433421	0.003144	2500	25	2419	14	2321	14	7.16
15Q22-2-56	314.66	401.36	0.78	0.159296	0.003452	9.071862	0.182905	0.410481	0.003633	2450	37	2345	19	2217	17	9.51
15Q22-2-57	221.95	287.04	0.77	0.166957	0.003130	11.101656	0.262789	0.475624	0.005747	2527	31	2532	22	2508	25	0.76
15Q22-2-58	89.27	720.14	0.12	0.168381	0.002837	9.050548	0.200400	0.386096	0.006168	2543	28	2343	20	2105	29	17.22
15Q22-2-59	29.49	126.48	0.23	0.163188	0.002712	8.520720	0.133607	0.376282	0.003038	2500	28	2288	14	2059	14	17.64
15Q22-2-63	52.24	1749.35	0.03	0.164190	0.004235	7.785736	0.310373	0.336474	0.008031	2499	44	2207	36	1870	39	25.18
15Q22-2-64	192.27	295.09	0.65	0.163193	0.003921	10.711688	0.396810	0.467821	0.008603	2500	40	2498	34	2474	38	1.04
15Q22-2-68	52.58	209.79	0.25	0.166341	0.002855	11.137268	0.184093	0.482154	0.003039	2521	29	2535	15	2537	13	-0.61
Later metamorphism or alteration events																
15Q22-2-01	440	3490	0.13	0.175600	0.003731	10.271794	0.211863	0.421447	0.003128	2613	35	2460	19	2267	14	13.24
15Q22-2-07	166	351	0.47	0.186552	0.003663	12.089244	0.265305	0.467514	0.004331	2712	32	2611	21	2473	19	8.83
15Q22-2-19	137	853	0.16	0.052924	0.001755	0.254823	0.008437	0.034663	0.000394	324	71	230	7	220	2	32.23
15Q22-2-28	161	915	0.18	0.062728	0.003256	0.327560	0.019946	0.036612	0.001071	698	111	288	15	232	7	66.80
15Q22-2-34	193	2131	0.09	0.150781	0.002568	7.713826	0.130920	0.368252	0.002839	2355	29	2198	15	2021	13	14.16
15Q22-2-35	231	427	0.54	0.142898	0.003575	6.738158	0.175553	0.339277	0.004217	2263	42	2078	23	1883	20	16.77
15Q22-2-36	115	695	0.16	0.050679	0.003205	0.239969	0.008150	0.035445	0.000428	233	146	218	7	225	3	3.80
15Q22-2-37	192	2029	0.09	0.046938	0.001227	0.165666	0.004199	0.025431	0.000238	56	50	156	4	162	1	-190.90
15Q22-2-41	145	1758	0.08	0.178978	0.003464	10.354317	0.193034	0.416638	0.002693	2644	32	2467	17	2245	12	15.07
15Q22-2-47	91.6	205	0.45	0.134951	0.002944	6.596173	0.210252	0.349427	0.006304	2165	43	2059	28	1932	30	10.76
15Q22-2-52	174	1945	0.09	0.186770	0.003344	11.512424	0.189273	0.444040	0.003972	2714	29	2566	15	2369	18	12.72
15Q22-2-65	91.9	130	0.71	0.132687	0.004025	4.042326	0.115521	0.220808	0.002867	2200	54	1643	23	1286	15	41.54
15Q22-2-67	149	1581	0.09	0.174891	0.002977	9.693961	0.162423	0.398585	0.002312	2605	28	2406	16	2163	11	16.99

Note: Degree of discordance = 100×(1−($^{206}Pb/^{238}U$ age/$^{207}Pb/^{206}Pb$ age)), $\lambda^{238}U = 0.0155125\times10^{-9}$ yr^{-1}, $\lambda^{235}U = 0.98485\times10^{-9}$ yr^{-1}, $\lambda^{232}Th = 0.049475\times10^{-9}$ yr^{-1}.